Electron Transfer Induces Side-Chain Conformational Changes of Glutamate-286 from Cytochrome bo 3 †

ARTICLE *in* BIOCHEMISTRY · MARCH 1999

Impact Factor: 3.02 · DOI: 10.1021/bi981859k · Source: PubMed

Electron Transfer Induces Side-Chain Conformational Changes of Glutamate-286 from Cytochrome bo_3[†]

Mathias Lübben,* Alexander Prutsch, Björn Mamat, and Klaus Gerwert

Lehrstuhl für Biophysik, Ruhr-Universität Bochum, Universitätsstrasse 150, D-44780 Bochum, Germany

Received August 3, 1998; Revised Manuscript Received November 30, 1998

ABSTRACT: Heme-copper oxidases have two putative proton channels, the so-called K-channel and the membrane-spanning D-channel. The latter contains a number of polar groups with glutamate-286 located in its center, which could—together with bound water—contribute to a transmembrane hydrogen-bonded network. Protonation states of carboxyl groups from cytochrome bo_3 of *Escherichia coli* were studied by redox Fourier transform infrared (FTIR) difference spectroscopy. A net absorbance increase in the carboxyl region was observed upon reduction. The band signature typically found in heme−copper oxidases comprises an absorbance decrease (reduced-minus-oxidized difference spectra) at 1745 cm^{-1} and increase at 1735 cm^{-1}. No significant changes in the carboxyl region were found in the site-specific mutants D135E and D407N. The difference bands were lacking in redox spectra of mutants at position 286; they could clearly be related to Glu-286. In wild-type oxidase, the p*K* of Glu-286 appears to be higher than 9.8. Upon solvent isotope exchange from H_2O to D_2O, the band at 1745 cm^{-1} shifts more readily than the one at 1735 cm^{-1}, indicating dissimilar accessibility of the carboxyl side chain to the hydrogen-bonded network in both redox states. The data are consistent with a redox-triggered conformational change of Glu-286, which attributes to the carboxyl group an orientation toward the interior of the D-channel for the oxidized form. The change of Glu-286 is retained in cyanide complexes of cytochrome bo_3 and of cytochrome *c* oxidase; therefore it should be related to oxidoreduction of the heme *b* and/or Cu_B metal centers.

Heme-copper oxidases are redox-driven proton pumps in the aerobic respiratory chain of microorganisms and mitochondria. The enzymes are integrally located in energy-transducing membranes and they belong to a protein superfamily comprising different subgroups that use either cytochrome *c* or quinols as donors of electrons, which are transferred to the terminal acceptor oxygen (*1*−*3, 55*). During the chemical process of oxygen reduction and water formation, protons are taken up from the cytoplasma (bacteria) or matrix (mitochondria). The free energy of the chemical reaction is sufficient to drive additional movement of protons across the membranes (*4, 5*). Recently the 3D structures of cytochrome *c* oxidases from mitochondria and from the proteobacterium *Paracoccus denitrificans* were solved (*6, 7*) to a level of 2.3 and 2.7 Å, respectively. The structural models of subunits I−III from both proteins are closely related but different in detail, which lead to fundamentally distinct mechanistic proposals of transmembrane proton translocation (*6, 8*−*9*). Amino acid sequences are very similar within the superfamily, and a number of strictly conserved residues have been predicted to be functionally relevant (*1, 3*). This was experimentally supported by numerous biochemical and biophysical data (for reviews, see refs *5* and *10*). It is therefore justified to regard the structures of cytochrome *c* oxidases as prototypes for the related ubiquinol oxidase cytochrome bo_3 of *Escherichia coli*. Structural models allow postulation of different proton translocating channels. One of these, the so-called K-channel, consists of the amino acids Lys-362, Thr-359, Thr-352, and Tyr-288 and ends at the binuclear heme-copper reaction center, which is located almost in the center of the membrane (*E. coli* enzyme numbering). Recent data ascribe to this half-channel a role in the first phase of the reaction cycle, when the enzyme accepts electrons and takes up two protons (*10, 11*). The D-channel is another array of charged or polar amino acids. In case of the bacterial oxidases it is proposed to have contact with both membrane surfaces (*8*). At the cytoplasmic side the entry is formed by Asp-135, Thr-201, and Asn-207; it comes via Glu-286 into close proximity with the binuclear reaction center, which binds dioxygen and forms the site of oxygen intermediate production during the catalytic reaction (*4*). Electrostatic calculations envision the binding of a few water molecules in this part of the channel (*12, 50*), whereas crystallographic data report the presence of only one bound water molecule (*7*). The exit half (on the periplasmic side) of the D-channel is less clear; a number of water molecules constituting a hydrogen-bonded network were detected recently in the channel outlet of *Paracoccus* enzyme. The network is possibly stabilized by propionic acid groups of heme *o* and by polar or acidic amino acid side chains (*7*) (Asp-407 and Asn-412 in the homologous *E. coli* enzyme). The recently published model of mitochodrial oxidase disagrees with the role of the D-channel and assumes an essentially different proton pathway implying the so-called "H-channel" (*6, 13*), ascribing a key role to the amino acid Asp-51 (bovine mitochondria numbering), which is, however, not conserved in the superfamily (*1, 3*).

[†]Supported by the Deutsche Forschungsgemeinschaft, Grant SFB 394-C6 to M.L.

* Corresponding author: Phone +49-700-4465; FAX +49-709-4626; e-mail luebben@bph.ruhr-uni.bochum.de.

10.1021/bi981859k CCC: $18.00
Published on Web 01/28/1999

On the basis of the bacterial model of proton pathways, both K- and D-channels are essential for catalysis during the oxygen reaction cycle by intimate cooperation, because site-directed mutations at either position (e.g., changes of Lys-362 in the K-channel or Glu-286 in the D-channel from charged to neutral side chains) severely affected oxidase activity and/or proton pumping competence (*11, 14, 15*). A crucial role of Glu-286 in the mechanism of proton conduction has been underlined (*16*). The existence of the same set of oxygen intermediates suggests that cytochrome *c* oxidases and the ubiquinol oxidase cytochrome bo_3 have similar reaction mechanisms (*17*−*19*). However, a recent report came up that suggests significant differences in both enzymes regarding the coupling of electron transport to possible mechanisms of transmembrane proton translocation (*20, 21*): the idea of a unique reaction mechanism in heme−copper oxidases has been challenged by enzymological and spectroscopic data, which led to the proposal of a Q-cycle mechanism being operative in quinol oxidases (*22*). This hypothesis would, of course, imply fundamental differences in the pathway of proton translocation in both types of oxidase. Anyway, experimental proofs would necessarily require a close comparison of cytochrome *c* and ubiquinol oxidase.

Metalloproteins undergoing valence-dependent optical changes could be readily investigated by redox difference spectroscopy. In extension of the classical reduced-minus-oxidized electronic difference spectroscopy, we developed a technique to study redox transients in the infrared spectral region (*23*). FTIR[1] spectroscopy is a powerful method for the detection of structural changes on the secondary and tertiary structure level as well as for the involvement of individual amino acid side chains during catalytic turnover (*43, 44*). To initiate the reaction, we used a "caged electron" technique, which employs flavin mononucleotide as an intermediate electron transmitter. After photochemical activation by ultraviolet laser light, the caged compound injects electrons liberated from the sacrificing donor EDTA into the redox centers of the cytochrome oxidase. This approach has led to the detection of absorbance differences in various heme-copper oxidases, including a prominent signature pattern with absorbance differences at 1745 and 1735 cm^{-1} (*23*).

In general, band assignments in infrared spectroscopy of proteins are made by use of either isotopic labeling or site-specific mutagenesis. In this report we assign the 1745/1735 signature band from cytochrome bo_3 of *E. coli* by means of site-specific mutants. It is concluded that the acidic amino acid side chain of Glu-286 undergoes a conformational change upon oxidoreduction, which may be an important step in the proton translocation process of this heme-copper oxidase.

MATERIALS AND METHODS

Expression and Purification of Wild-Type and Mutagenized Cytochrome bo_3. Cytochrome bo_3 from *Escherichia coli* was expressed from either the plasmid pHTAG or pHCL

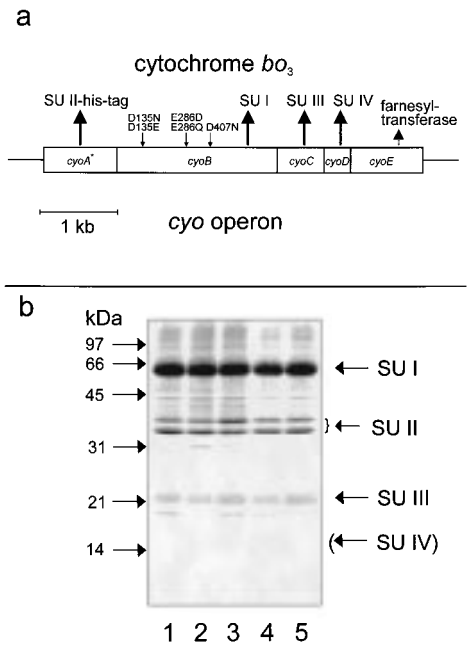

FIGURE 1: (a) Structure of the *cyo* operon. The structural genes and the corresponding gene products are shown (bigger arrows). The mutagenized amino acids in subunit I (CyoB) are presented in the one-letter code by arrows pointing to the respective codon positions. (b) SDS−15% polyacrylamide gel electrophoresis of wild-type and mutant proteins, which are oligohistidine-tagged at the C-terminus of subunit II. Seven micrograms of protein was loaded per lane: lane 1, wild-type cytochrome bo_3; lanes 2−5, mutant proteins (2) E286D, (3) E286Q, (4) D407N, and (5) D135E.

(the latter is a kind gift of Dr. Anne Puustinen, Helsinki), both pBR322 derivatives carrying the *cyo* operon (*24*). In the pHTAG construct the *cyoD* gene is genetically modified by a DNA fragment encoding an oligohistidine tag at the C-terminus of subunit IV for easier purification on a metal affinity column. The pHCL plasmid encodes a C-terminal oligohistidine extension in *cyoA* (*25*); it is related to pHTC8 (26) and we verified the presence of all cysteine codons by DNA sequencing. Both pHTAG and pHCL plasmids are regarded to encode the "wild-type" protein. We constructed site-specific mutants, based on pHCL, with respect to positions Glu-286, Asp-135, and Asp-407 (Figure 1a). Nucleotides were replaced by the PCR "overlap extension" method (*27, 28*). The mutagenized 1.5 kb *Sal*I−*Nsi*I fragments of the *cyoB* gene were moved into pHCL, and insertions were verified by DNA sequencing. As an assay of proton pumping activity in vivo we tested the ability of mutagenized plasmids to complement the respiratory defect of a *cyo* and *cyd* double deletion strain, *E. coli* JM107ΔΔ. For the purpose of enzyme preparation, wild-type and mutant cytochrome bo_3 were expressed in the *cyo* deletion strain *E. coli* BL21Δ*cyo*.

After solubilization with a mixture of *n*-octyl β-D-glucoside and Triton X-100, proteins were purified by batch elution with 100 mM imidazole at pH 8.0 from Ni-NTA-agarose columns. After buffer exchange to 20 mM Tris-HCl, 0.3% *n*-decyl β-D-maltoside, pH 8.0, the samples were concentrated as in ref *23*. Details of the molecular genetic and protein chemical procedures will be published elsewhere. Cytochrome *c* oxidase of *Rhodobacter sphaeroides* was a kind gift of Antony Warne and Professor Matti Saraste, Heidelberg. Protein determination was performed spectroscopically

[1] Abbreviations: FTIR, Fourier transform infrared. The amino acid positions of heme-copper oxidases are numbered according to the sequence of the CyoB gene product (= subunit I) of *Escherichia coli* in the three-letter-code, except for designation of site-specific mutants, where the one-letter-code was used.

(*52*) and polyacrylamide gel electrophoresis was done as described in ref *53*.

Duroquinol Oxidase Activity Assay. The activity of cytochrome bo_3 was tested with the synthetic analogue duroquinol (=2,3,5,6-tetramethylbenzoquinol in its chemically reduced form was a kind gift from Professor Oettmeier, Bochum). The medium consisted of 50 mM phosphate buffer, pH 7.0, 1 mM EDTA, 0.3% *n*-decyl β-D-maltoside, 0.2 mg/mL phosphatidylcholine vesicles, and 0.2 mM duroquinol. The absorbance difference $\Delta A_{270-285}$ (*29*) was followed in an SLM-Aminco DW-2 spectrophotometer at room temperature after addition of 0.25 μg of purified oxidase; the autoxidation rates determined after addition of 0.5 mM KCN were subtracted.

Sample Preparation for Spectroscopy. Samples were prepared with minor modifications as described in ref 23: 2−3 μL of oxidase solution in a buffer of 20 mM Tris-HCl and 0.3% *n*-decyl β-D-maltoside, pH 8.0, was combined with 0.8 μL of a solution consisting of 0.5 mM flavin mononucleotide and 100 mM EDTA, if not indicated otherwise. For investigation of the cyanide effect, 0.5 μL of 200 mM KCN was added to the sample. The mixture was spread out on a CaF_2 plate, and a thin hydrated film was formed after further concentration for 3−4 min with a vacuum pump.

FTIR Spectroscopy. Redox FTIR difference spectra were taken on a Bruker IFS66v spectrometer as described in ref *23*. If not indicated differently, infrared intensity transmitted by a low-pass filter cutting at 1950 cm^{-1} was measured; the nominal resolution of spectra was 4 cm^{-1}. For better comparison of different samples and for the calculation of double difference spectra as in ref *30*, absorbance difference bands were normalized within the spectral regions of 1130−1540 cm^{-1} or of 1695−1705 cm^{-1}. If not pointed out otherwise in figure legends, spectra are normalized to the 1695−1705 cm^{-1} region of wild-type cytochrome bo_3 (in Tris-HCl, pH 8.0, in H_2O) and are presented as an average of 2000 scans.

RESULTS

Biochemical Properties of Mutants. The putative D-channel of cytochrome oxidases known to be proton-pumping has three conserved amino acids with negatively charged side chains (*3*, *8*). These are located at the entry (Asp-135) and exit (Asp-407) sites and in an internal position next to the enzyme's reaction center (Glu-286). These residues were assumed to be functionally important. Site-specific amino acid replacements at positions 135 and 407 did not alter the enzyme activity in vivo, as shown by the capability of the respective mutant plasmids to complement a respiratory-deficient host strain *E. coli* JM107ΔΔ (Table 1). Removal of negative charge at position 135 leads to the formation of microcolonies, which may indicate a lowered effectiveness of this cytochrome bo_3 mutant. Glu-286 is strictly conserved in the pumping oxidases. This points to a key role of its carboxyl side chain being correctly positioned for transmembrane proton translocation. The change of Glu-286 to a noncharged amino acid fatally affects the activity of the enzyme (Table 1). This is in contrast to the mutant E286D, which forms a catalytically active oxidase proficient at restoring proton pumping in vivo. The presence of a carboxyl side chain at this position appears to be essential for the function of cytochrome bo_3, which also has been reported by others (*14*−*16*).

Table 1: Characterization of Cytochrome bo_3 Mutants

cytochrome bo_3	plasmid complementation of respiratory deficiency[a]	duroquinol oxidase activity[b] ($e \cdot s^{-1}$)	% of control
none (pSTAG)[c]	−		
wild type (pHCL)[d]	+	88 ± 2	100
E286D	+	86 ± 9	98
E286Q	−	14 ± 2	16
D407N	+	70 ± 5	80
D135N	(+)[e]	nd	
D135E	+	86 ± 14	98

[a] The plasmids encoding wild-type or mutagenized cytochrome bo_3 were transformed into strain *E. coli* JM107ΔΔ, which has no aerobic respiration due to genomic deletions of the genes for cytochrome bo_3 and *bd* and does not grow overnight on LB agar plates. When the strain was complemented with genes encoding functional cytochrome bo_3 oxidase, growth was restored and colonies were formed on plates. [b] Duroquinol oxidase activity was tested with purified cytochrome bo_3, $n = 3$. [c] Negative control, the *cyo* genes with a partial deletion of *cyoB* (Δ*Bgl*II fragment) are cloned into plasmid pSTAG (based on pBR322); no cytochrome bo_3 is produced from that strain. [d] Positive control, pHCL carries the *cyo* genes (modified as outlined in the Materials and Methods section). [e] Microcolonies much smaller than wild type were formed. The D135N mutant did not express enough cytochrome bo_3 for purification and activity tests.

Wild-type and mutant cytochrome bo_3 extended by oligohistidine at the C-terminus of subunits II or IV were expressed and purified by metal affinity chromatography. All samples were pure as judged by polyacrylamide gel electrophoresis and retained their four subunits (Figure 1b). Room-temperature optical difference spectra (reduced-minus-oxidized) of wild-type and mutagenized enzymes listed in Table 1 had maxima at 426 and 562 nm. For unknown reasons, cytochrome bo_3 of the mutant D135N was expressed to such a low level that purification was ineffective. The enzyme function of site-specifically altered enzymes was investigated by measuring the oxidation rates of the artificial substrate duroquinol. Activity data of purified oxidases are consistent with the in vivo assay (Table 1), which demonstrates that mutants at positions 135 and 407 have almost wild-type characteristics, whereas the mutant E286Q is strongly disfigured.

Redox FTIR Experiments of Cytochrome bo_3. Photoreduction of oxidases was performed in situ; ultraviolet laser light has been used to initiate the electron transfer from flavin mononucleotide. As an example, Figure 2 shows how the redox transients of wild-type oxidase evolve by increasing number of absorbed photons. The protein concentration in the thin sample films was adjusted to the maximum in order to achieve a high signal-to-noise ratio in the carboxyl region. Compared with earlier results (*23*), transmission is lower in the amide I to II region at wavenumbers lower than 1680 cm^{-1}. Figure 2 exhibits the same "up-and-down"-patterns observed earlier in various heme−copper oxidases (*23*), the one of *E. coli* being placed at 1664 cm^{-1} (maximum)−1657 cm^{-1} (minimum)−1653 cm^{-1} (maximum)−1649 cm^{-1} (minimum). Thus, redox-induced polypeptide backbone changes concluded earlier to take place from experiments with dilute samples are likewise detectable with this highly concentrated sample form.

After 200−300 laser flashes, complete reductive turnover of cytochrome bo_3 is achieved as jugded by its electronic absorbance spectra recorded before and after photoreduction, which are identical to the optical spectra obtained from fully

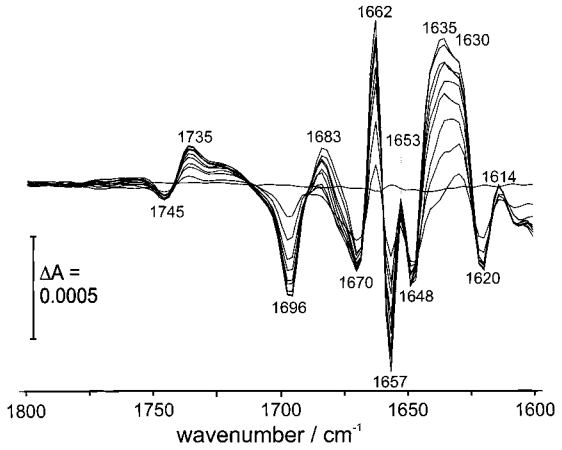

FIGURE 2: Redox FTIR spectrum of wild-type cytochrome bo_3. The oxidized sample (oligohistidine-tagged at C-terminus of subunit II) was mixed with the caged electron donor flavin mononucleotide and photoreduced at room temperature with 308 nm irraditation by a UV laser. After a package of 20 flashes (approximately 20 mJ/pulse) at 0.1 Hz repetition rate, 400 scans were co-added; this program was repeated 9 times. The light-induced evolution of reduced-minus-oxidized absorption difference spectra is displayed; positive (negative) bands correspond to absorbances of the reduced (oxidized) form.

oxidized and dithionite-reduced samples in free solution (not shown). Initially the photoreduction progresses proportional to the number of applied flashes, indicating that almost no oxygen is present in the sample films. The courses of flash-dependent reactions measured at different wavenumbers in the carboxyl region could be fitted with hyperbolic functions (data not shown); photoreduction at the different wavenumbers appears to be monophasic with respect to the number of executed laser flashes.

The presence of isosbestic points at 1740, 1710, and 1690 cm^{-1} (Figure 2) argue for a transition between two states in the carboxyl region, i.e., above 1690 cm^{-1}. No evidence for possible intermediates, as found by an electrochemical equilibration technique (*31*), is observed. During photoreduction the wild-type enzyme develops absorbance differences at 1735 cm^{-1} (absorbance increase) and 1745 cm^{-1} (absorbance decrease) (Figure 2). The formation of both bands appears to correlate roughly, suggesting that the underlying processes are coupled. The observed amplitudes are probably different due to additional absorbance contributions of other groups.

Mutants at Position Glu-286. Figure 3 displays FTIR absorbance difference spectra of wild-type cytochrome bo_3 and of site-specific mutants at position Glu-286 from 1690 to 1800 cm^{-1}. In this spectral region, carbonyl groups of amino acid side chains and propionic acid chains of porphyrins absorb (*32*−*34*, *45*). The spectra are displayed as photoreduced-minus-oxidized difference, with positive (negative) bands being attributed to the reduced (oxidized) state.

The zero level of difference spectra is outlined by the spectral region between 1800 and 1780 cm^{-1} (Figure 2) further extending up to 1900 cm^{-1} (not shown), where no significant absorbance changes are developed during photoreduction. All samples exhibit a negative absorbance difference band at 1696 cm^{-1} irrespective of the solvent isotope. Wild-type cytochrome bo_3 (Figure 3a) produces a band pattern that has been regarded as signature for proton-pumping heme-copper oxidases, namely, a negative absorbance band at 1745 cm^{-1} and a positive absorbance band at 1735 cm^{-1} (*23*). An additional shoulder could be resolved at 1720−1725 cm^{-1} under the present experimental conditions (see spectra with 2 cm^{-1} nominal resolution in Figure 5). If equilibrated to the solvent D_2O (Figure 3b), the band maximum shifts from 1735 to 1727 cm^{-1}, whereas the minimum is broadened from 1745 to 1736 cm^{-1}. Band positions between 1680 and 1750 cm^{-1} *plus* their sensitivity to solvent isotope exchange are indicative for C═O stretching vibrations of protonated carboxyl groups. These signals disappear upon deprotonation and formation of the anionic state.

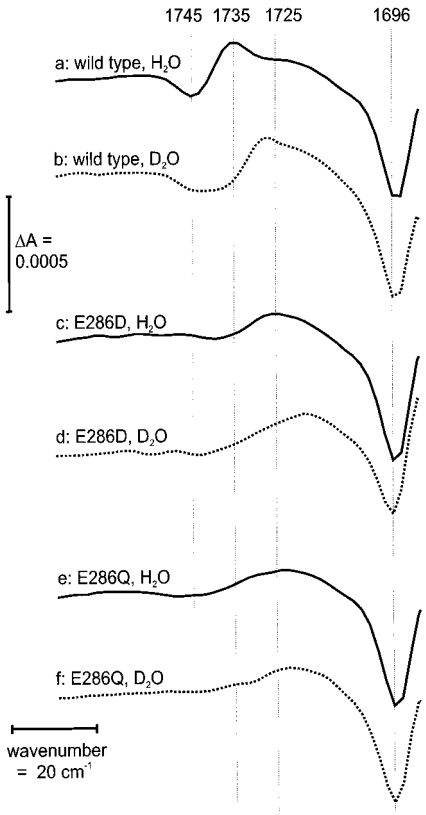

FIGURE 3: Redox FTIR absorbance difference spectra of the carbonyl region of purified cytochrome bo_3 and mutants with respect to Glu-286, oligohistidine-tagged at subunit II. Spectra were recorded from sample dissolved in H_2O (solid lines) or D_2O (dotted line). (a, b) Wild type; (c, d) E286D mutant; (e, f) E286Q mutant.

The signature pattern disappears in the mutant E286D (Figure 3c), in which the carboxylic acid side chain is shortened by one CH_2 group. The residual positive difference peak of 1725 cm^{-1} shifts to 1718 cm^{-1} upon solvent exchange (Figure 3d). It is important to note that the isopolar E286D replacement is not invasive to the protein, because the cytochrome bo_3 function remains unaltered.

In the isosteric but biologically nonfunctional mutant E286Q the charged side chain is abolished, but a broad positive absorbance band centered at about 1725 cm^{-1} remains. Upon D_2O-H_2O exchange this band shifts by about 4 cm^{-1} to lower wavenumbers.

Subtraction of the two redox difference spectra, wild type-minus-E286Q (Figure 3a,e), yields the double difference spectrum presented in Figure 4. The broad band component at about 1725 cm^{-1} disappears in the double difference spectrum, i.e., the involved functional group(s) contribute-(s) to the net increase of absorbance, which is not caused by Glu-286. A residual pattern of two difference bands with

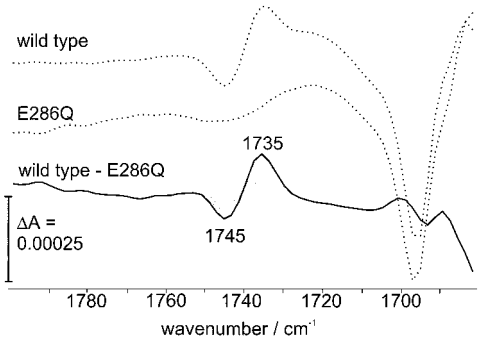

FIGURE 4: Double difference redox FTIR spectra of wild-type cytochrome bo_3 and mutant E286Q. For clarity, the redox difference spectra already shown in Figure 3 (a and e) are displayed again with dotted lines. Normalization of spectra with respect to (i) the absorbance regions between 1705 and 1695 cm^{-1}, (ii) between 1300 and 1470 cm^{-1}, and (iii) between 1130 and 1540 cm^{-1} came to almost identical results, demonstrating double difference bands with a minimum at 1745 cm^{-1} and maximum at 1735 cm^{-1} assigned to Glu-286.

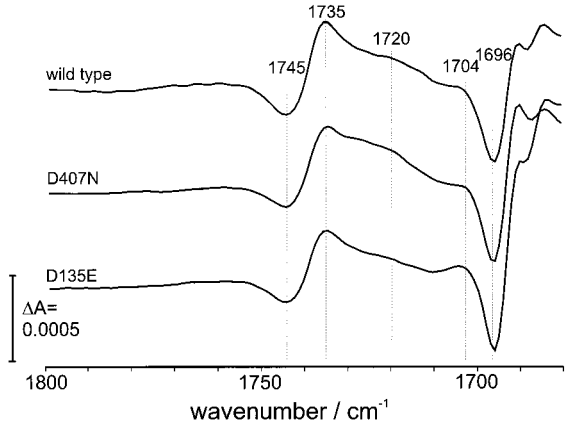

FIGURE 5: Redox FTIR absorbance difference spectra of the carbonyl region of purified cytochrome bo_3 and mutants with respect to Asp-135 and Asp-407 (subunit II tagged). The nominal spectral resolution is 2 cm^{-1}. (Top) Wild type; (middle) D407N mutant; (bottom) D135E mutant.

maximum at 1735 cm^{-1} and minimum at 1745 cm^{-1} demonstrates that *both signals* are most likely related to the carboxyl side chain of Glu-286. The areas of these two bands are of comparable size (Figure 4). Similar results are obtained when double difference spectra of wild type-minus-E286D are calculated (not shown).

Mutants at Positions Asp-135 and Asp-407. To get more detailed information about the groups contributing to the carboxyl region, redox difference spectra at higher resolution (2 cm^{-1}) were recorded (Figure 5). The control experiment with wild-type enzyme confirms the 1745/1735 difference pattern known from lower resolution spectra (see above). An increase of integral band intensity between 1700 and 1740 cm^{-1} provides evidence for net protonation increase upon reduction. The broad feature appears to be composed of more than one band, because one recognizes the reproducibly occurring shoulders at 1720 and 1704 cm^{-1}. Solvent isotope exchange to D_2O induces band shifts of the 1745/1735 pattern to smaller wavenumbers as expected. The composite broad peak shifts correspondingly in D_2O medium, but no fine structure is resolved (data not shown), leaving assignments of the 1704 and 1720 cm^{-1} absorptions to carboxyl groups rather premature. In addition, Figure 5 shows

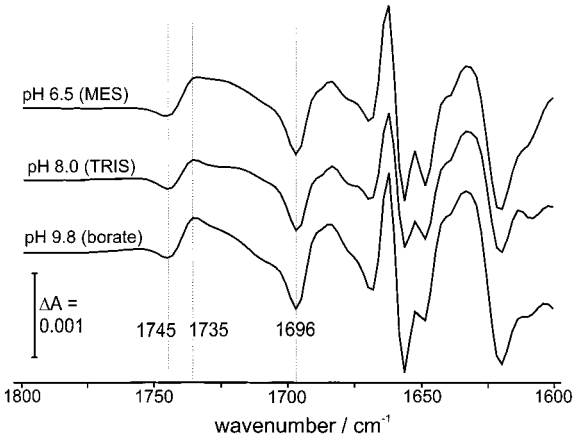

FIGURE 6: Redox FTIR absorbance difference spectra of purified cytochrome bo_3 (tagged at subunit IV) equilibrated to different buffers at various pH values: 20 mM *N*-morpholinoethanesulfonic acid (MES), pH 6.5 (top); 20 mM Tris-HCl, pH 8.0 (middle); and 20 mM sodium borate, pH 9.8 (bottom).

the spectra of the D135E and D407N mutants, at which loss or shift of difference bands would be expected in the carboxyl region. Static redox difference spectra of both mutants closely resemble the one obtained from wild type; thus carboxyl side chains of the respective amino acids do not contribute to changes induced by electron transfer under conditions of this experiment.

Accessibility to Solvent and Protons. Redox spectra were measured at different pH values in order to obtain a rough figure of the p*K*s of carboxyl groups contributing to the absorbance difference spectrum. Equilibration to the desired pH values was verified by demonstrating band shifts by solvent isotope exchange to D_2O. Difference spectra are remarkably similar in the range of pH 6.5−9.8, irrespective of cytochrome bo_3 expression from pHTAG (Figure 6) or pHCL (not shown). The p*K* values of carboxyl groups involved in the absorbance changes therefore appear to be higher than 9.8. The oxidase seems to be fairly tolerant to slightly alkaline conditions. Duroquinol oxidase activity could be measured only up to pH 8.5, where rates are still at 80% of maximum at pH 7.5.[2]

The accessibility of carboxyl groups to solvent molecules was probed by H_2O/D_2O exchange. Samples were equilibrated to different extents by exposure to the solvent for different periods. After brief incubation (about 5 h) in D_2O (Figure 7b) the negative absorbance band at 1745 cm^{-1} remains, while the positive absorbance at 1735 cm^{-1} is partly shifted to 1727 cm^{-1}. This shift is completed after longer exposure to D_2O [about 2 days (Figure 7c)]. The negative absorbance band at 1745 cm^{-1} is broadened significantly. Double difference spectra from samples dissolved in H_2O and D_2O (Figure 7, spectra b − c and 7 a − c) clearly show a positive band at 1735 cm^{-1} and a minor negative feature at 1727 cm^{-1}, indicating that the signal at 1735 cm^{-1} alone is sensitive to isotope exchange. The absence of an expected negative band demonstrates that solvent equilibration does not affect the carboxyl group absorbing at 1745 cm^{-1}.

Redox Behavior of the Cyanide Complex of Cytochrome bo_3. The oxidase inhibitor cyanide binds to the ferric high-

[2] Measurement of duroquinol oxidase activity at pH values higher than 8.5 is rather imprecise due to rapid autoxidation of the substrate.

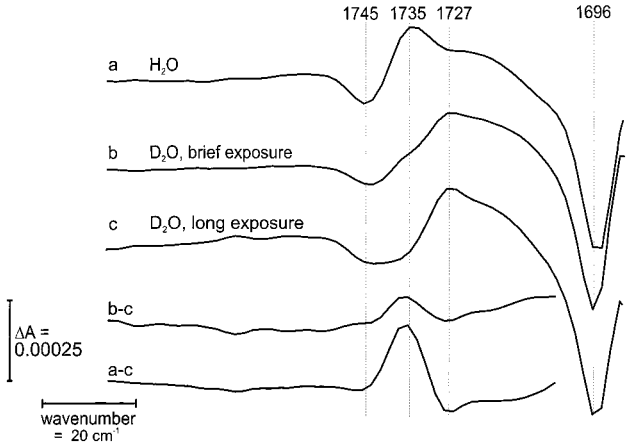

FIGURE 7: Redox FTIR absorbance difference spectra of purified wild-type cytochrome bo_3 at pH 8.0 (tagged at subunit II) equilibrated to different extents to D_2O. Solvent exchange was done by repeated (i) 20-fold dilution of the oxidase solution with Tris buffer made up in D_2O and (ii) spin concentration with Microcon 30 tubes. After the procedure was finished, an FTIR sample was prepared from the concentrate and the redox spectrum was measured after about 5 h (brief exposure, spectrum b). Another FTIR sample was prepared from the same concentrate 2 days later and was measured as above (long exposure, spectrum c). The control (sample in H_2O) is shown in spectrum a.

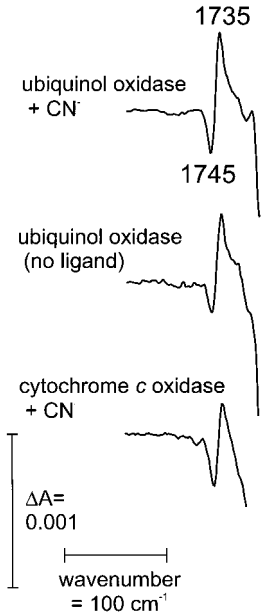

FIGURE 8: Effect of cyanide on redox FTIR difference spectra of cytochrome bo_3 and of cytochrome aa_3. The infrared intensity transmitted through a low-pass filter cutting at 2600 cm^{-1} was measured; the spectral resolution was 2 cm^{-1}. (Top) Cytochrome bo_3 plus KCN; (middle) cytochrome bo_3 without KCN; (bottom) cytochrome aa_3 plus KCN.

spin heme *o* of cytochrome bo_3 or heme *a* of cytochrome aa_3. In the cyanide-complexed form, reduction of the bound Fe^{3+} center is strongly inhibited. It is thus possible to investigate whether heme *o*/*a* is involved in the development of the carboxyl difference pattern at 1745/1735 cm^{-1}. The complex formation of cyanide with the enzymes was verified by measuring the decrease of the absorbance band of the bridging complex at 2147 cm^{-1} for cytochrome bo_3 (*35*) and of 2153 cm^{-1} for cytochrome *c* oxidase (*36*) (not shown) during photoreduction of the enzyme−ligand complexes. Redox difference spectra of both types of heme-copper oxidase are independent of the presence of cyanide (Figure 8). Thus, the redox state of high-spin heme *o* or *a* is not directly responsible for the induction of changes that give rise to the carboxyl difference band pattern.

DISCUSSION

By use of a photochemical reduction technique, redox difference spectra were recorded in the carbonyl absorption range of cytochrome bo_3. Carbonyl groups could be assigned by their frequency and bandshifting to smaller wavenumbers of about 8 cm^{-1} after H_2O/D_2O exchange. The carboxyl group of Glu-286 clearly contributes to the absorbance changes observed in redox difference FTIR spectra, because the 1745/1735 cm^{-1} signal pattern is lost upon replacement of this amino acid by the isopolar aspartate and the isosteric glutamine. The disappearance of both the positive and the negative difference band allows us to assign the carboxyl group. Only in its undissociated form does the C═O bond of carboxylic acids absorb in the range of 1680−1760 cm^{-1}; i.e., Glu-286 must be protonated at least in some stage of the photoreaction (see below). From band assignments by an FTIR study on CO flash photolysis of cytochrome bo_3, it became definitively known that the carboxyl group of Glu-286 absorbs at about 1726−1731 cm^{-1} (at the temperature of 80 K) and therefore it is protonated in the reduced state (*26*). The positive difference band at 1735 cm^{-1} (Figures 2 and 3a) thus clearly originates from Glu-286. In fact, the static redox spectra represent the difference of fully reduced minus fully oxidized forms of the enzymes. From structural models we can extract information about the protonation state in the oxidized protein: The homologue of Glu-286 is most likely in the neutral form of azide-bound *P. denitrificans* oxidase (=Glu-278) (*7*) or has been noted to be neutral in crystals of oxidized as well as of reduced beef heart mitochondrial oxidase (=Glu-242) (*6*). If the oxidase is protonated in the structures of reduced *and* oxidized proteins, it is clearly inferred that the negative absorbance difference band at 1745 cm^{-1} (Figures 3a and 4) is not from a deprotonation reaction of another carboxyl group but must also originate from Glu-286 itself. Independence of the 1745/1735 cm^{-1} band pattern in redox spectra up to pH 9.8 strongly argues for a very high proton affinity of Glu-286. The relatively high wavenumbers of the 1745/1735 cm^{-1} pattern plead for a carboxyl group in the protein interior effectively shielded from extensive hydrogen bonding of the solution state.

In the oxidized state, a carboxyl group location in a more hydrophobic environment would result in the negative band. This is further underlined by the absence of $^1H/^2H$ exchange for the more hydrophobic environment of Glu-286, indicating nonaccessibility for water in the oxidized state (Figure 7), where the side chain should be disconnected from the binuclear reaction center (see below). Conversely, Glu-286 has access to solvent (protons) in the reduced enzyme, when it is in aequous contact with the binuclear reaction center (*12*, *26*). The positive FTIR absorbance band found at 1735 cm^{-1} would then be caused by a more hydrophilic environment of the residue. Gradual lowering of proton mobility in space, from channel entrance to the gate, would be an important feature expected for proton pumps in order to avoid proton slipping. Assumed that Glu-286 is directly involved in a proton conduction mechanism (*12*) gated via the binuclear

reaction center (*37, 38*), the side-chain orientation to different hydrogen-bonded environments would be very plausible.

The 1735/1745 cm^{-1} band pattern of the catalytically active E286D mutant would be anticipated to slightly shift to higher wavenumbers, if one solely considers spectra of free glutamic and aspartic acid (*32*). The lack of the wild-type spectral signature without appearance of a novel band pattern indicates that Asp-286 would stay either protonated or unprotonated irrespective of the redox state of the protein. Earlier FTIR spectroscopic investigations of CO photolysis (*26*) revealed unexpected behavior of the mutant E286D, which exhibits a significant upshift to ca. 1760 cm^{-1}. It has been assumed (*26*) that glutamic and aspartic acid at position 286 adopt different alignments relative to the hydrogen-bonded network within the D-channel. With respect to FTIR redox difference spectra, these distinct orientations may as well explain the presence of the 1745/1735 cm^{-1} pattern for the wild type and its unexpected absence for the E286D mutant.

Similar observations regarding the involvement of carboxyl groups have been made with the cytochrome *c* oxidase of the soil bacterium *Paracoccus denitrificans* (*31*). For this oxidase the difference pattern at 1746/1734 cm^{-1} has been assigned to the homologue of Glu-286; it gets lost upon substitution with glutamine or aspartic acid (*31*). A possible contribution of the amino acid side chains corresponding to Asp-135 and Asp-407 to the (fully reduced minus fully oxidized) redox difference FTIR signals could be excluded as well. In both oxidases, the carboxyl groups involved in the redox-driven absorbance changes in the 1746/1734 cm^{-1} region appear to have relatively high p*K* values (>8.7), not unexpected for carboxyl groups that are deeply buried within the membrane dielectric (*54*). However, carefully determined titration curves of both enzymes are necessary for a detailed discussion of p*K* values with respect to the difference bands related to Glu-286. Taken together, the results suggest that the overall structural and functional similarity of ubiquinol and cytochrome *c* oxidases could in principle be extended also to the pathway of protons across the cytoplasmic membrane.

Due to the distinct nature of substrates of both oxidases (cytochrome *c* is barely an electron donor, whereas ubiquinol is an electron *plus* a proton donor), one should admit certain differences at least in some steps of transmembrane proton translocation. The data recorded in ref *31* were obtained by an electrochemical equilibrium method. In addition to the 1746/1734 cm^{-1} redox difference signal pattern, the authors report a pair of difference bands absorbing at 1738/1728 cm^{-1} only at intermediate redox potentials. On the other hand, transient bands different from the ones discussed already were not detectable by the photoreduction procedure applied in this work. The stepwise transfer of electrons by virtue of flavin mononucleotide chemistry is not an equilibrium technique. Our photochemical spectra do not provide evidence for the existence of intermediate bands in cytochrome bo_3 of *E. coli*, since homogeneous difference bands are formed, which exhibit isosbestic points in the carbonyl region (Figure 2). Similar results were obtained with the cytochrome *c* oxidase *of Rhodobacter sphaeroides*, which is closely related to the *Paracoccus* enzyme (M.L., unpublished data; *23*). It is possible that the occurrence of an extra pair of bands in ref *31* is inherent to the electrochemical technique itself or perhaps is due to the fact that a fraction of the oxidase molecules stays in a different functional state (e.g., the "resting state"). Interestingly, the negative 1746 cm^{-1} band can be shifted by 4−6 cm^{-1} upon $^2H-^1H$ exchange in the *Paracoccus* enzyme, which is in obvious contrast to our observations on cytochrome bo_3 (Figure 7) and may be another indication for the different functional behavior of cytochrome *c* and ubiquinol oxidase. Due to the band heterogeneity at ≈1735 cm^{-1}, found with the electrochemical equilibration technique (*31*), scenarios of more than a singular carboxyl group accounting for the observed band pattern at 1746/1734 cm^{-1} cannot be fully ruled out for the *Paracoccus* enzyme.

No carboxyl groups are located in the postulated K-channel of mitochondrial and bacterial cytochrome *c* oxidases (*8, 9*). Owing to their close sequence similarity, most probably this holds as well for the cytochrome bo_3 of *E. coli*. The presence of a net positive absorbance shifting to smaller wavenumbers after solvent exchange to D_2O (Figure 3a,b) indicates that carboxyl groups other than Glu-286 are protonated in the reduced form of cytochrome bo_3. This is especially evident from the broad positive band of the E286Q and E286D mutants, where contributions from Glu-286 are eliminated. The involvement of carboxyl groups in redox-linked protonation changes thus allows an insight into the mechanism of proton translocation within the D-channel of cytochrome bo_3 or, alternatively, of the "H-channel" (*13*) suggested recently to be operative in the mitochondrial oxidase. The static FTIR redox difference spectra allow us to assign the initial and the final states of the enzyme reaction with the substrate dioxygen, namely, the fully reduced and oxidized states of the oxidase. Upon reduction of the fully oxidized enzyme, protons are considered to be taken up from the cytoplasmic side via the K- but not via the D-channel (*10*). The overall absorbance increase in the region of 1720−1725 cm^{-1} observed experimentally by redox FTIR spectroscopy may be related to net proton uptake. This could be explained by intramolecular proton transfer, either via K-channel or resulting from delocalized protons loaded before into the hydrogen-bonded network of the D-channel. Substrate and pumped protons of heme−copper oxidases are translocated in the oxidative half of the reaction cycle (*14*) following binding of dioxygen to the fully reduced enzyme, especially during the partial reactions from the peroxy → oxyferryl and the oxyferryl → oxidized states, that have been attributed as the proton pumping steps (*39*). Possible candidates for protonation changes that have in part been demonstrated to be involved in proton translocation are the *conserved* aspartates, 135 (*40*) and 407, but none of the investigated mutants exhibit other than wild-type (static) redox difference spectra in the carboxyl region. Biochemical and structural data emphasize the flexibility of the hydrogen-bonded network at the entry and exit sites of the D-channel (*7, 41*), allowing us to predict alternative pathways of proton conduction for this local sector. Heme propionyl side chains could be protonated (*34*) but could not be assigned in the carbonyl region above 1700 cm^{-1} for the *Paracoccus* oxidase (*42*). Other as yet unidentified carboxyl groups could further contribute. Due to the lack of conservation of aspartate-51 of the mitochondrial cytochrome *c* oxidase (*6*), it is difficult to assess whether a functional equivalent of it might exist in bacteria.

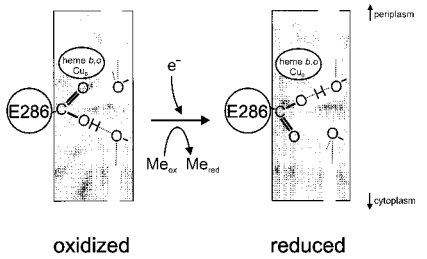

FIGURE 9: Possible schematic model explaining protonation states of carboxyl groups in the transmembrane D-channel of cytochrome bo_3. Two hydrogen-bonded networks representing input and output halves of D-channel located below and above Glu-286 are schematically drawn as bent stripes. The binuclear reaction center is included to specify the spatial orientation. The direction of the observed photoreaction (oxidized → reduced) is indicated by the arrow; metal centers (Me_{ox} → Me_{red}) take up the electrons. Fully reduced and fully oxidized enzymes represent the initial and the final state of the enzyme during catalytic reaction; these are defined by the static FTIR redox difference spectra. The model shows the redox-induced conformational change of Glu-286, by which its carboxylic side chain is positioned into environments of distinct hydrophobicity. The side-chain conformational change forms a path between both hydrogen-bonded networks. See text for further details.

Upon reduction, protons could also be taken up directly from the medium, perhaps involving carboxyl groups exposed to the protein surface. Recent electrostatic calculations provided evidence for a possible engagement of the conserved Glu-78 (subunit II of *P. denitrificans*) in proton uptake coupled to binuclear center reduction (*46*). Interestingly, its carboxyl side chain is located close to the K-channel residues and may control the delivery of protons to the reaction center. Site-specific mutants in cytochrome bo_3 at this position with only 10% of wild-type catalytic activity have been created (R. B. Gennis, personal communication); the results underline that also residues from other subunits may be important for proton pumping.

Our redox FTIR data on cytochrome bo_3 are summarized in a model describing the change of protonation states allocatable to the reduced and oxidized enzyme (Figure 9). It assumes Glu-286 is fully protonated in both the reduced and oxidized forms. Glu-286 senses electrostatic changes of the (reduced) Cu_B center probably mediated by bound water molecules (*12, 26*); therefore the carboxyl side chain should be connected to the binuclear reaction center in the reduced enzyme. Protons would be translocated in the intermediate state(s), coupled to a reorientation of the environment of Glu-286 or to a *conformational change* of the carboxyl group itself. The side chain of Glu-286 moves from a relatively hydrophobic position facing away from the binuclear center (weaker hydrogen bonding, oxidized state) to another, more hydrophilic orientation located closer to the reaction center (stronger hydrogen bonding, reduced state). Intermediate protonation changes of Glu-286 are possible but could not be resolved by static FTIR spectroscopy. This model is in line with the existence of the 1745/1735 band pattern and would readily explain the lack of a corresponding band signature in the E286Q mutant.

The crucial role of Glu-286 for transmembrane proton translocation has already been emphasized in earlier studies. Its carboxyl side chain is either directly or indirectly involved in protonation changes within the D-channel. In fact, recently performed theoretical calculations of possible energy states based on different methods predict fairly drastic side-chain conformational changes of Glu-286 (*49, 50*). The conformational change postulated from the spectroscopic data could, however, be a very subtle reorientation of the carboxyl side chain into an environment of different hydrophobicity. At current resolutions of structural models of oxidized and reduced enzymes (*6, 7*), this change may even be invisible with X-ray techniques.

In this context it is interesting to note that the protonated carboxyl group of Asp-96 (with a p$K > 9$) has a key role in the proton uptake pathway of the light-driven proton pump bacteriorhodopsin (*47, 56*). Proton-transfer implying bound water molecules takes place via a hydrogen-bonded network extending through the proton channel (*48*). It seems that hydrogen-bonded proton transfer in combination with a catalytically involved protonated carboxyl group within a relatively hydrophobic environment are common features of proton-transfer mechanisms found in at least one group of non-evolutionarily-linked membrane proteins (*48, 51*).

At present, no direct conclusions on the mechanism of H^+ pumping of cytochrome oxidase can be drawn, because different scenarios are conceivable. These would imply proton conduction in intermediate steps involving the bimetallic reaction center as proposed in the "histidine-cycling" hypothesis (*38*), and would still allow coupling to a gross conformational change involving an H-channel as suggested from high-resolution structural data (*6*).

Not all redox centers of cytochrome oxidase appear to be equally involved in the redox-driven conformational change. We can clearly exclude Cu_A, which is not present in cytochrome bo_3. The insensitivity of the Glu-286 conformational change to the binding of cyanide to heme *o* (or a_3 in cytochrome *c* oxidase) further excludes the respective metals. The relevant redox transition sensed by Glu-286 is therefore restricted to either heme *b* (or *a* in cytochrome *c* oxidase), Cu_B , or both of these metals. For the *Paracoccus* cytochrome *c* oxidase the redox transition of heme *a* has been suggested to be coupled to formation of the difference pattern of the glutamic acid homologous to Glu-286 (*31*).

The schematic model presented here (Figure 9) summarizes our interpretation for the experimental data observed by redox FTIR spectroscopy and provides a basis for future studies. In addition to the need for assigning the residual carboxyl signals it will be especially substantial to study the redox kinetics of cytochrome bo_3 for a better understanding of the catalytic mechanism. It is very important to carry out a thorough investigation of the pH dependence of the redox difference spectra, because electron-transfer-associated p*K* changes of Glu-286 and other carboxyl groups contributing to the hydrogen-bonded network will be crucial for the understanding of the enzyme function. After the recent emergence of data suggesting the possible existence of a Q cycling mechanism in ubiquinol oxidase (*21*), the comparison of proton translocation mechanisms in the different heme−copper oxidases cytochrome bo_3 and cytochrome aa_3 will be of particular importance.

ACKNOWLEDGMENT

We are grateful to Dr. Benedikt Hessling and Dr. Mårten Wikström for stimulating discussions and to Mrs. Iris Schönhaar for excellent technical assistance.

REFERENCES

1. Saraste, M. (1990) *Q. Rev. Biophys. 23*, 331−366.
2. Lübben, M. (1995) *Biochim. Biophys. Acta 1229*, 1−22.
3. Garcia-Horsman, J. A., Barquera, B., Rumbley, J., Ma, J., and Gennis, R. B. (1994) *J. Bacteriol. 176*, 5587−5600.
4. Babcock, G. T., and Wikström, M. (1992) *Nature (London) 356*, 301−309.
5. Ferguson-Miller, S., and Babcock, G. T. (1996) *Chem. Rev. 96*, 2889−2907.
6. Yoshikawa, S., Shinzawa-Itoh, K., Nakashima, R., Yaono, R., Yamashita, E., Inouye, N., Yao, M., Fei, M. J., Libeu, C. P., Mizushima, T., Yamaguchi, H., Tomizaki, T., and Tsukihara, T. (1998) *Science 280*, 1723−1729.
7. Ostermeier, C., Harrenga, A., Ermler, U., and Michel, H. (1997) *Proc. Natl. Acad. Sci. U.S.A. 94*, 10547−10553.
8. Iwata, S., Ostermeier, C., Ludwig, B., and Michel, H. (1995) *Nature 376*, 660−669.
9. Tsukihara T., Aoyama, H., Yamashita, E., Tomizaki, T., Yamaguchi, H., Shinzawa-Itoh, K., Nakashima, R., Yaono, R., and Yoshikawa, S. (1996) *Science 272*, 1136−1144.
10. Brzezinski, P., and Ädelroth, P. (1998) *J. Bioenerg. Biomembr. 30*, 99−107.
11. Ädelroth, P., Gennis, R. B., and Brzezinski, P. (1998) *Biochemistry 37*, 2470−2476.
12. Riistama, S., Hummer, G., Puustinen, A., Dyer, R. B., Woodruff, W. H., and Wikström, M. (1997) *FEBS Lett. 41*, 275−280.
13. Gennis, R. B. (1998) *Science 280*, 1712−1713.
14. Ädelroth, P., Svensson-Ek, M., Mitchell, D. M., Gennis, R. B., and Brzezinski, P. (1997) *Biochemistry 36*, 13824−13829.
15. Konstantinov, A. A., Siletsky, S., Mitchell, D., Kaulen, A., and Gennis, R. B. (1997) *Proc. Natl. Acad. Sci. U.S.A. 94*, 9085−9090.
16. Verkhovskaya, M. L., Garcia-Horsman, A., Puustinen, A., Rigaud, J.-L., Morgan, J. E., Verkhovsky, M. I., and Wikström, M. (1997) *Proc. Natl. Acad. Sci. U.S.A. 94*, 10128−10131.
17. Morgan, J. E., Verkhovsky, M. I., Puustinen, A., and Wikström, M. (1995) *Biochemistry 34*, 15633−15637.
18. Svensson-Ek, M., Thomas, J. W., Gennis, R. B., Nilsson, T., and Brzezinski, P. (1996) *Biochemistry 35*, 13673−13680.
19. Svensson-Ek, M., and Brzezinski, P. (1997) *Biochemistry 36*, 5425−5431.
20. Musser, S. M., Stowell, M. H. B., Lee, H. K., Rumbley, J. N., and Chan, S. I. (1997) *Biochemistry 36*, 894−902.
21. Schultz, B. E., Edmondson, D. E., and Chan, S. I. (1998) *Biochemistry 37*, 4160−4168.
22. Musser, S. M., Stowell, M. H. B., and Chan, S. I. (1993) *FEBS Lett. 327*, 131−136.
23. Lübben, M., and Gerwert, K. (1996) *FEBS Lett. 397*, 303−307.
24. Au, D. C.-T., and Gennis, R. B. (1987) *J. Bacteriol. 169*, 3237−3244.
25. Rumbley, J. N., Nickels, E. F., and Gennis, R. B. (1997) *Biochim. Biophys. Acta 1340*, 131−142.
26. Puustinen, A., Bailey, J. A., Dyer, R. B., Mecklenburg, S. L., Wikström, M., and Woodruff, W. H. (1997) *Biochemistry 36*, 13195−13200.
27. Ho, S. N., Hunt, H. D., Horton, R. M., Pullen, J. K., and Pease, L. R. (1989) *Gene 77*, 51−59.
28. Tomic, M., Sunjevaric, I., Savtchenko, E. S., and Blumenberg, M. (1990) *Nucleic Acids Res. 18*, 1656.
29. Zweck A., Bechmann, G., and Weiss, H. (1989) *Eur. J. Biochem. 183*, 199−203.
30. Brudler, R., de Groot, H. J., van Liemt, W. B., Steggerda, W. F., Esmeijer, R., Gast, P., Hoff, A. J., Lugtenburg, J., and Gerwert, K. (1994) *EMBO J. 13*, 5523−5530.
31. Hellwig, P., Behr, J., Ostermeier, C., Richter, O. M. H., Pfitzner, U., Odenwald, A., Ludwig, B., Michel, H., and Mäntele, W. (1998) *Biochemistry 37*, 7390−7399.
32. Venyaminov, S. Y., and Kalnin, N. N. (1990) *Biopolymers 30*, 1243−1257.
33. Tamm, L. K., and Tatulian, S. A. (1997) *Q. Rev. Biophys. 30*, 365−429.
34. Contzen, J., and Jung, C. (1998) *Biochemistry 37*, 4317−4324.
35. Tsubaki, M., Mogi, T. Anraku, Y., and Hori, H. (1993) *Biochemistry 32*, 6065−6072.
36. Yoshikawa, S., Mochizuki, M., Zhao, X.-J., and Caughey, W. S. (1994) *J. Biol. Chem. 270*, 4270−4279.
37. Wikström, M., Bogachev, A., Finel, M., Morgan, J. E., Puustinen, A., Raitio, M., Verkhovskaya, M., and Verkhovsky, M. I. (1994) *Biochim. Biophys. Acta 1187*, 106−111.
38. Morgan, J. E., Verkhovsky, M. I., and Wikström, M. (1994) *J. Bioenerg. Biomembr. 26*, 599−608.
39. Wikström, M. (1989) *Nature (London) 338*, 776−778.
40. Thomas, J. W., Puustinen, A., Alben, J. O., Gennis, R. B., and Wikström, M. (1993) *Biochemistry 32*, 10923−10928.
41. Mitchell, D. M., Fetter, J. R., Mills, D. A., Ädelroth, P., Pressler, M. A., Kim, Y., Aasa, R., Brzezinski, P., Malmström, B., Alben, J. O., Babcock, G. T., Ferguson-Miller, S., and Gennis, R. B. (1996) *Biochemistry 35*, 13089−13093.
42. Behr, J., Hellwig, P., Mäntele, W., and Michel, H. (1998) *Biochemistry 37*, 7400−7406.
43. Gerwert, K. (1993) *Curr. Opin. Struct. Biol. 3*, 769−773.
44. Mäntele, W. (1993) *Trends Biochem. Sci. 18*, 197−202.
45. Buchanan, S., Michel, H., and Gerwert, K. (1992) *Biochemistry 31*, 1314−1322.
46. Kannt, A., Lancaster, R. D., and Michel, H. (1998) *Biophys. J. 74*, 708−721.
47. Gerwert, K., Hess, B., Soppa, J., and Oesterhelt, D. (1989) *Proc. Natl. Acad. Sci. U.S.A. 86*, 4943−4947.
48. Rammelsberg, R., Huhn, G., Lübben, M., and Gerwert, K. (1998) *Biochemistry 37*, 5001−5009.
49. Pomès, R., Hummer, G., and Wikström, M. (1998) *Biochim. Biophys. Acta 1365*, 255−260.
50. Hofacker, I., and Schulten, K. (1998) *Proteins: Struct., Funct., Genet. 30*, 100−107.
51. Wikström, M. (1998) *Curr. Opin. Struct. Biol. 8*, 480−488.
52. Kita, K., Konishi, K., and Anraku, Y. (1984) *J. Biol. Chem. 259*, 3368−3374.
53. Laemmli, U. K. (1970) *Nature (London) 227*, 680−685.
54. Bashford, D., and Gerwert, K. (1992) *J. Mol. Biol. 224*, 473−486.
55. Saraste, M., Holm, L., Lemieux, L. J., Lübben, M., and van der Oost, J. (1991) *Biochem. Soc. Trans. 19*, 608−612.
56. Gerwert, K., Souvignier, G. and Hess, B. (1990) *Proc. Natl. Acad. Sci. U.S.A. 87*, 9774−9778.

BI981859K